



Research paper

Numerical simulation study on mechanical properties of rock like specimen with cracks under the coupling of loading and unloading and osmotic pressure

Liangxiao Xiong¹, Haijun Chen², Zhongyuan Xu³, Deye Hu⁴

Abstract: The saturated metasandstone is taken as the research object, and the uniaxial compression characteristics of the saturated metasandstone are simulated by means of the artificially made saturated sandstone samples. By checking the parameters of the Particle Flow Code (PFC) numerical simulation of loading and unloading seepage stress coupling, the effects of the conductivity coefficient, the pipe diameter, the apparent volume of the domain and the time step on the calculation results are analyzed. When PFC is used for numerical simulation of seepage stress coupling, the conductivity coefficient K can be taken as 0.010. When the pipe diameter is 1.0 mm, the apparent volume of the current domain is $1 \times 10^{-6} \text{ m}^3$, the water pressure distribution inside the sample is relatively uniform. The influence of time step on the compressive strength and peak strain of the specimen can be almost ignored. Under the action of water pressure, the compressive strength of the intact rock like sample and the rock like sample with cracks decreases, and the compressive strength of the sample decreases gradually with the increase of water pressure. When the inclined angle of fracture is the same, the seepage pressure is the same, and the confining pressure is the same, the compressive strength of the specimen also increases with the increase of the initial axial stress level during unloading. When the confining pressure and the osmotic pressure are the same, the unloading effect makes the crack development of the specimen faster and more complete, the specimen is more fragmented and multiple parallel shear bands develop.

Keywords: rock like specimen, seepage stress coupling, compressive strength

¹Associate Prof., PhD., Eng., School of Civil Engineering and Architecture, East China Jiaotong University, Nanchang 330013, China, e-mail: xionglx1982@126.com, ORCID: 0000-0002-6366-5187

²Prof., PhD., Eng., Geotechnical Engineering Department, Nanjing Hydraulic Research Institute, Nanjing, 210029, China, e-mail: hjchen@nhri.cn, ORCID: 0000-0003-0094-9649

³PhD, Faculty of Geosciences and Environmental Engineering, Southwest Jiaotong University, Chengdu 611756, China, e-mail: zyxu@swjtu.edu.cn, ORCID: 0000-0003-4303-1870

⁴BEng., School of Civil Engineering and Architecture, East China Jiaotong University, Nanchang 330013, China, e-mail: 2573713909@qq.com, ORCID: 0000-0001-8132-0812

1. Introduction

Groundwater often exists in actual rock mass engineering. Therefore, the mechanical properties of rock under the coupling action of seepage and stress have always been the focus of rock mechanics.

Besuelle *et al.* [1] conducted a laboratory experimental study of the hydromechanical behavior of boom clay, and found that the permeability of Boom Clay depend on the mean effective stress. Zhang *et al.* [2] carried out experimental study of the hydro-mechanical behaviour of the Callovo-Oxfordian argillite, and found that the gas permeability parallel to the bedding plane is about one order of magnitude higher than that perpendicular to the bedding. Yang *et al.* [3] carried out a series of tests including uniaxial compression and dehydration and hydration at different constant applied stress levels, and found that the shrinkage and swelling depend on the applied stress and the angle with respect to the vertical direction of the mechanical load and the stratification plane. Yu *et al.* [4] investigated the mechanical properties and permeability variation in single joint rock samples filled with a gypsum layer, the results indicated that the peak strength and failure modes change with the inclined angles.

The above researchers mainly studied the mechanical properties of rock under the coupling action of loading stress and seepage. In actual rock mass engineering, loading and unloading are caused by excavation, so it is more necessary to study the mechanical characteristics of rock under the coupling action of loading and unloading and seepage.

Ning *et al.* [5] performed a series of tests to study the mechanical properties of granite subjected to triaxial cyclic loading-unloading compression under hydro-mechanical coupling, and the results show that the damage and permeability evolution of rock are interrelated. Liu *et al.* [6] conducted triaxial compression tests with progressive unloading of confining pressure upon sandstone specimens under different combinations of initial confining pressures and pore pressures, and found that the magnitude of initial confining pressure and pore pressure influences significantly the rock strength, energy conversion, crack propagation, and dilatancy during unloading process. Chen *et al.* [7] conducted a series of triaxial tests with permeability and acoustic emission signal measurement under the path of confining pressure unloading prior to the peak stress, and found that under the confining pressure unloading conditions, a good correspondence relationship among the stress-axial strain curve, permeability-axial strain curve and acoustic emission activity pattern is obtained. Zhang *et al.* [8] studied permeability characteristics of broken coal and rock under cyclic loading and unloading, and the laboratory test results imply that permeability stress sensitivity and permeability loss of the first loading and unloading were significantly greater than the succeeding cyclic loading and unloading. Zhang *et al.* [9] analyzed the permeability changes of rock samples in the process of reloading to failure after unloading at different stages, and found that the permeability of rock samples loaded after unloading at different stages is different under the condition of residual strength.

At present, many researchers mainly carry out indoor tests on the mechanical properties of rock specimens under the coupling action of loading and unloading stress and seepage, while the research results on the numerical simulation of the mechanical properties of rock under the coupling action of loading and unloading stress and seepage have not been reported in the literature. Therefore, in this paper, the saturated metasandstone is taken as the research

object, and the uniaxial compression characteristics of the saturated metasandstone are numerically simulated through the artificially made saturated sandstone samples. By checking the parameters of the PFC numerical simulation of loading and unloading seepage stress coupling, the influence of the conductivity coefficient, pipe diameter, apparent volume of the domain and time step on the calculation results is analyzed, and the values of the conductivity coefficient, pipe diameter, apparent volume of the domain and time step are finally determined. Through numerical simulation, the effects of seepage pressure and initial axial stress level on the compressive strength and crack evolution were analyzed.

2. Numerical model and determination of meso parameters of rock like materials

2.1. Research object

Taking the metamorphic sandstone of the deep buried extra long tunnel as the reference object, cement, barite powder, water, poly carboxylic acid super plasticizer, etc. are used to make the rock like materials. Through the uniaxial compression test and numerical simulation of the rock like materials under the saturated state, the mesoscopic parameters of the saturated samples during the numerical simulation are determined.

425 Portland cement were used as the cement and medium standard sand were used as the sand when making the sample. The specimen is a cylindrical specimen with a diameter of 50 mm and a height of 100 mm. Finally, it is determined that the mass of cement, barite powder, sand, water and water reducer is 3.17 kg, 1.90 kg, 2.86 kg, 1.59 kg and 0.48 kg respectively for every 10 kg of the complex.

2.2. Fracture combination form

The length of cracks in all samples is 20 mm and the thickness of cracks is about 2 mm. Inclined angle β of prefabricated crack is the angle between the prefabricated crack and the horizontal line, and the inclined angle β includes 5 kinds, i.e. 0° , 30° , 45° , 60° and 90° . The schematic diagram of inclined angle β of prefabricated crack of 45° is shown in Fig. 1.

2.3. Determination of meso parameters of saturated samples

Triaxial test and meso numerical simulation are carried out for the rocks under the saturated state. The values of meso parameters of the intact samples under the saturated state are shown in Table 1.

Comparison of test and numerical simulation results of triaxial compression stress-strain curve of saturated specimen is shown in Fig. 2. Comparison of test and numerical simulation results of fracture mode is shown in Fig. 3.

The uniaxial compressive strength and elastic modulus of the specimen obtained from the test are 25.21 MPa and 5.32 GPa, respectively. The uniaxial compressive strength and

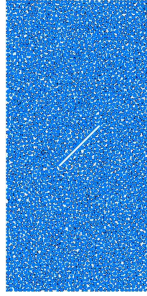


Fig. 1. The schematic diagram of inclined angle β of prefabricated crack of 45°

Table 1. Meso parameters of intact specimen under saturated condition

| Particle contact Modulus (GPa) | Tangential stiffness ratio of particle | Friction coefficient of particle | Density of particle (kg/m^3) | Porosity | Average normal strength of parallel bonding (MPa) | Average tangential strength of parallel bonding (MPa) |
|--------------------------------|--|----------------------------------|---|----------|---|---|
| 5.0 | 1.6 | 0.18 | 2700 | 0.08 | 23.32 | 10.05 |

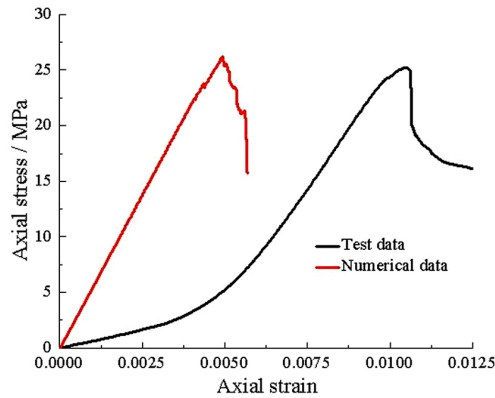


Fig. 2. Comparison of test results and numerical simulation results of triaxial compression stress-strain curves of saturated specimens

elastic modulus of the sample obtained from the numerical simulation are 26.02 MPa and 6.08 GPa, respectively. When conducting uniaxial compression tests, the initial porosity of the sample introduces an upper concave segment in the stress-strain curve. However, this upper concave segment is not observed in the numerical simulation. Consequently, disparities may arise in the peak strain of the stress-strain curve derived from experimental and numerical data. Microscopic parameters become applicable when the compressive strength and elastic

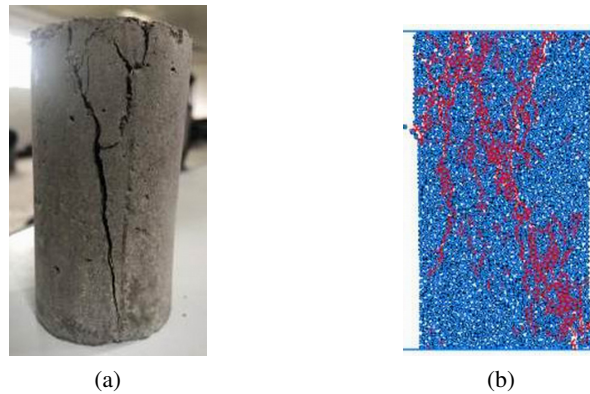


Fig. 3. The schematic diagram of inclined angle β of prefabricated crack of 45° : (a) Test results, (b) numerical simulation results

modulus obtained from both experiments and numerical simulations exhibit relative proximity. Therefore, the established numerical model and meso parameters can be used to further carry out the meso numerical simulation under the coupling of loading and unloading and osmotic pressure on the specimen with cracks.

3. Sensitivity analysis and parameter determination of fluid meso parameters

The fluid flow algorithm of PFC2D regards the crack between adjacent particles as a seepage pipe to simulate the fluid flow. During the hydraulic coupling test, the pipe network model is established for hydraulic coupling numerical simulation. When selecting the hydraulic coupling calculation model, in addition to the determination of the particle contact model and the corresponding meso parameters, it is also necessary to study the influence of the fluid meso parameters on the model. At present, there are few studies on how to determine the fluid meso parameters and parameter sensitivity analysis under the hydraulic coupling of particle flow program, and the determination of the fluid meso parameters is very critical in the simulation study of seepage failure, hydraulic fracturing and rock mass damage under hydraulic action.

The PFC built-in Fish language is used to program the coupling of conventional mechanical loading, unloading, and seepage. The simulation experiment of loading, unloading, and seepage coupling is achieved by controlling the movement of the wall.

During hydraulic coupling numerical simulation experiments, hydraulic gradients are added to the PFC biaxial system based on hydraulic coupling theory. The basin range and initial seepage pressure are preset, establishing an overall initial basin pressure of 0.1 MPa to reflect the saturated state of rock immersion. At the beginning of the biaxial compression test, pore water pressure is applied to the top of the specimen, and water head pressures of 1 MPa, 4 MPa,

and 7 MPa are applied to the top basin. This creates a head pressure difference vertically in the specimen, initiating the coupling between conventional loading and seepage. Throughout the hydraulic coupling test process, it is required for the numerical simulation specimen to reach a steady flow state at small strains, so the axial pressure loading speed should be moderated to avoid excessive velocity. In this test, strain control is used to maintain a constant loading rate at 0.02 mm/104 time steps. During the experiment, the model's stress-strain, crack distribution and quantity, water pressure distribution, macroscopic failure, and energy dissipation are monitored and recorded, enabling a comprehensive and intuitive analysis of the impact of hydraulic coupling on the mechanical properties of fractured rock masses.

In this paper, the flow pipe network is used for hydraulic coupling. Before the simulation, it is necessary to determine the influence of fluid parameters on the macroscopic mechanical characteristics of the sample, analyze the influence of four fluid calculation parameters (conductivity coefficient, pipe diameter, apparent volume of the domain, time step) on the compressive strength, peak strain and elastic modulus of the sample, and compare with the test results of other people. Finally, the fluid meso parameters suitable for the numerical model test in this paper are determined. During sensitivity analysis of fluid meso parameters, the values of basic meso parameters of model particles are shown in Table 2.

Table 2. Basic meso parameters of model particles when sensitivity analysis of fluid meso parameters is carried out

| Contact modulus of particle (GPa) | Normal tangential stiffness ratio of particle | Friction coefficient of particle | Density of particle (kg/m^3) | Average normal strength of parallel bonding (MPa) | Average tangential strength of parallel bonding (MPa) |
|-----------------------------------|---|----------------------------------|---|---|---|
| 5.4 | 1.5 | 0.3 | 2600 | 32.5 | 18.5 |

3.1. Conductivity

In the hydraulic coupling simulation test of PFC2D program, the fluid flow velocity is defined by the conductivity coefficient. In order to study the influence of flow velocity on the strength and stability of the model, the value range of the conductivity coefficient during the simulation is $0.002 \div 0.012$ m/s. The confining pressure is 10 MPa, the osmotic pressure is 5 MPa, and the other parameters are consistent. The influence of the conductivity coefficient on the stress-strain curve of the sample is shown in Fig. 4.

When the conductivity coefficient is too large, for example, when k is taken as 0.012, the "water flow" inside the sample is too fast, and the instantaneous water pressure is too large, which will cause the internal force imbalance and lead to the model imbalance, and the reasonable results cannot be obtained.

When the conductivity coefficient k is 0.010, the model will not be unstable and reasonable results can be obtained. When the conductivity coefficient k is 0.008, the compressive strength

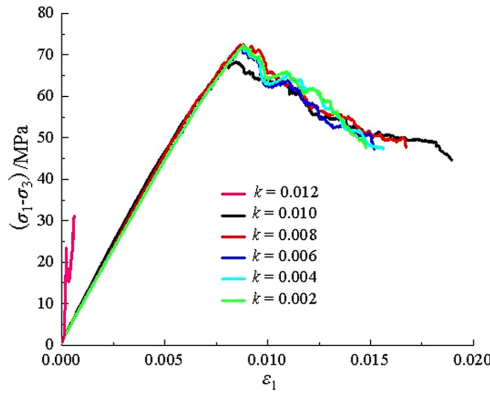


Fig. 4. Effect of conductivity on stress-strain curve of specimen

of the sample is greater than the compressive strength of the conductivity coefficient k is 0.010. When the conductivity coefficient k is continuously reduced, the compressive strength of the sample does not change significantly. The smaller the conductivity coefficient, the more the permeability of the sample decreases, and the strength will increase. When the conductivity coefficient k is smaller than 0.010, the conductivity had little effect on the elastic modulus of the sample.

The influence of the conductivity coefficient on the fracture mode of the specimen is shown in Fig. 5.

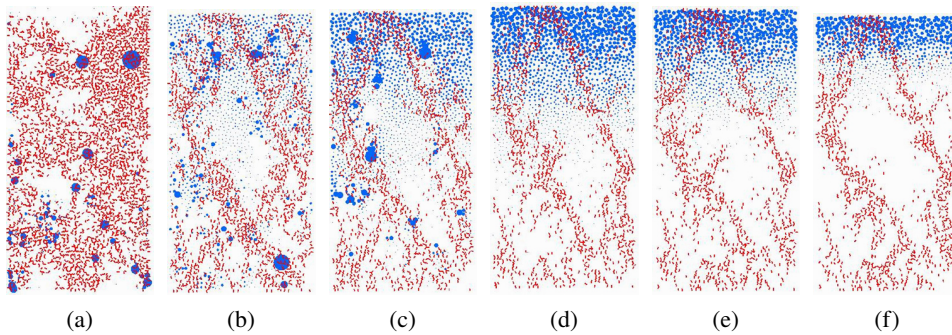


Fig. 5. Effect of conductivity on fracture mode of specimen: (a) $k = 0.012$, (b) $k = 0.010$, (c) $k = 0.008$, (d) $k = 0.006$, (e) $k = 0.004$, (f) $k = 0.002$

In Fig. 5, the red broken line indicates the crack, and the blue round ball indicates the water pressure. When the conductivity coefficient k is 0.012, 0.010, 0.008, 0.006, 0.004 and 0.002, the number of cracks in the sample is 3013, 1743, 1381, 1223, 1194 and 1198 respectively. The larger the conductivity coefficient is, the faster the fluid inside the sample will conduct to the whole, resulting in greater local water pressure inside the sample, more cracks and instability of the model.

According to the results in Fig. 4 and Fig. 5, when the PFC is used for numerical calculation, the conductivity coefficient k can be taken as 0.010.

3.2. Pipe diameter

The pipe diameter, that is, the opening of the fluid channel, has an initial opening during the construction of the fluid network to ensure that the fluid can flow when the particles are in close contact. In the case of cracking, the pipe diameter can represent the opening of the crack. In the numerical simulation calculation in this paper, the value range of pipe diameter is 0.01–2.5 mm, the confining pressure is 10 MPa, the osmotic pressure is 5 MPa, and the other parameters are consistent. The influence of pipe diameter on the stress-strain curve of the sample is shown in Fig. 6, and for the influence of pipe diameter on the fracture mode of the sample is shown in Fig. 7.

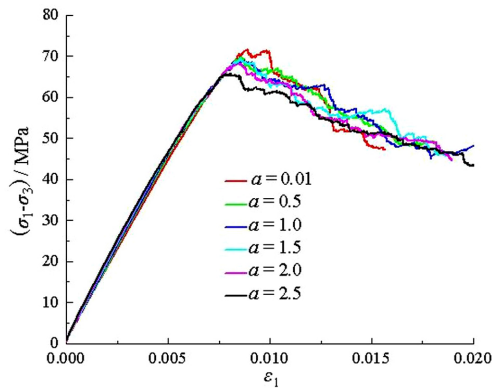


Fig. 6. Influence of pipe diameter on stress-strain curve of specimen

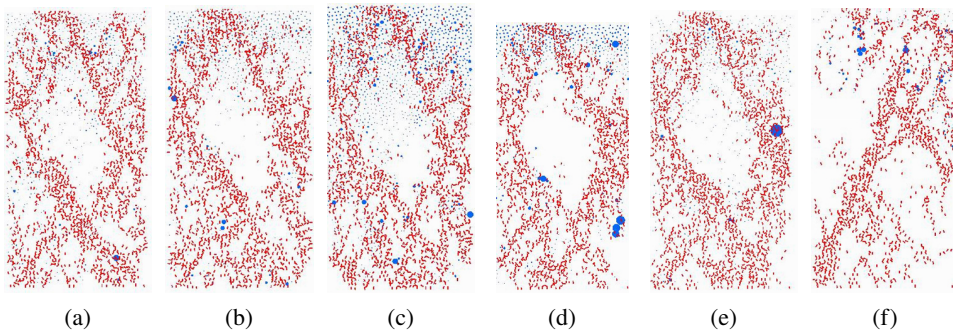


Fig. 7. Effect of pipe diameter on fracture mode of specimen: (a) $a = 0.01$, (b) $a = 0.5$, (c) $a = 1.0$, (d) $a = 1.5$, (e) $a = 2.0$, (f) $a = 2.5$

In Figure 7, the red broken line indicates the crack, and the blue round ball indicates the water pressure.

When the pipe diameter decreases, the compressive strength of the sample gradually increases. The smaller the pipe diameter is, the weaker the seepage capacity of the sample is, and the influence of water pressure superposition on the sample is reduced. When the

pipe diameter is 0.5 ~2.0 mm, the pipe diameter has little influence on the strength of the sample. When the pipe diameter is 1.0 mm, the water pressure distribution inside the sample is relatively uniform.

3.3. Apparent volume of domain

“Domain” represents the size of the water storage space of the fluid domain in the hydraulic coupling basin network, and the apparent volume of “domain” represents the fluid volume stored in the fluid domain.

In this paper, when the numerical simulation is carried out, and the value range of the apparent volume of the domain in the time is $2 \times 10^{-4} \div 1 \times 10^{-6} \text{ m}^3$, the confining pressure is 10 MPa, the osmotic pressure is 5 MPa, and other parameters are consistent. The effect of the apparent volume of the domain on the stress-strain curve of the specimen is shown in Fig. 8, and the effect of the apparent volume of the domain on the fracture mode of the specimen is shown in Fig. 9.

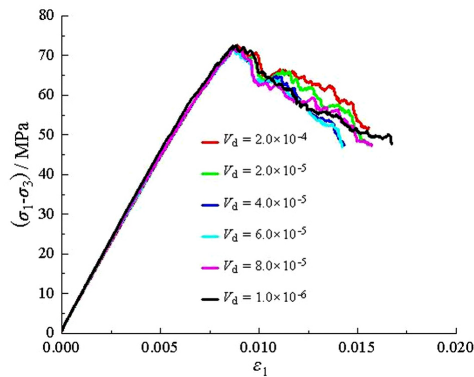


Fig. 8. Effect of apparent volume of domain on stress-strain curve of specimen

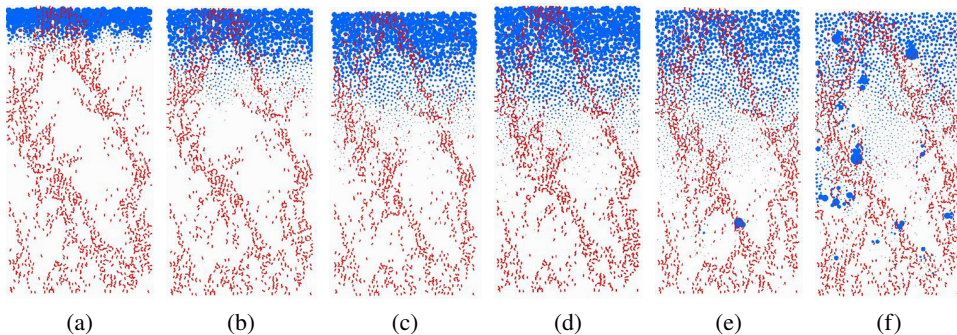


Fig. 9. Effect of apparent volume of domain on fracture mode of specimen: (a) $V_d = 2 \times 10^{-4} \text{ m}^3$, (b) $V_d = 2 \times 10^{-5} \text{ m}^3$, (c) $V_d = 4 \times 10^{-5} \text{ m}^3$, (d) $V_d = 6 \times 10^{-5} \text{ m}^3$, (e) $V_d = 8 \times 10^{-5} \text{ m}^3$, (f) $V_d = 1 \times 10^{-6} \text{ m}^3$

In Fig. 9, the red broken line indicates the crack, and the blue round ball indicates the water pressure. The value of the apparent volume of the domain has no obvious effect on the compressive strength and peak strain. When the value of the apparent volume of the domain is $1 \times 10^{-6} \text{ m}^3$, the water pressure distribution inside the sample is relatively uniform. Therefore, the apparent volume of the domain can be taken as $1 \times 10^{-6} \text{ m}^3$.

3.4. Time step

The time step represents the duration of each operation step in the hydraulic coupling process. The minimum critical time step needs to be determined during calculation to ensure that the global time step taken by the model is less than the critical time step. The closer the global time step is to the critical time step, the higher the calculation efficiency. If the time step is larger than the critical step, the particles in the model will be ejected, resulting in the failure of the model and cannot be calculated.

The value range of time step is $0.8 \times 10^{-4} \div 1.2 \times 10^{-4} \text{ s}$, confining pressure is 10 MPa, osmotic pressure P is 5 MPa, and other parameters are consistent. The effect of time step on the stress-strain curve of the sample is shown in Fig. 10.

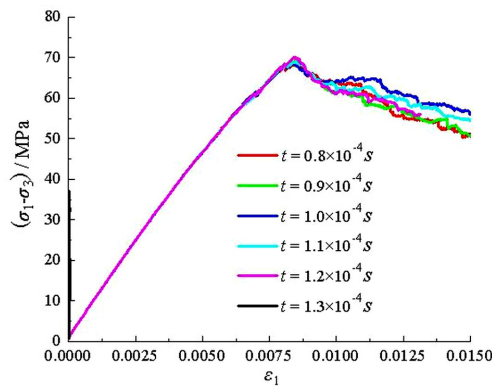


Fig. 10. Effect of time step on stress-strain curve of specimen

The influence of time step on the peak strength and peak strain of the specimen can be almost ignored.

3.5. Verification of numerical simulation of parameter value

Liu *et al.* [10] conducted triaxial unloading seepage coupling test on sandstone. The reliability of the particle flow program and relevant numerical model parameters was verified by simulating the deviator stress-axial strain curves of Liu *et al.* [10].

When simulating the deviator stress-axial strain curves of Liu *et al.* [10], the values of the basic meso parameters of particles and the hydraulic coupling meso parameters are shown in Table 3 and 4.

Table 3. The basic mesoscopic parameters of particles when simulating the deviator stress-axial strain curves of Liu et al. [10]

| Parameter name | Contact modulus of particle (GPa) | Friction coefficient | Density (kg/m ³) | Friction angle of parallel bonding (°) | Mean normal strength of parallel bonding (MPa) | Mean tangential strength of parallel bonding (MPa) |
|----------------|-----------------------------------|----------------------|------------------------------|--|--|--|
| Fish symbol | ba_Ec | ba_Fric | ba_rho | Pb_phi | Pb_sn_mean | Pb_ss_mean |
| Analog value | 4.5 | 0.15 | 2600 | 48 | 55.0 | 28.3 |

Table 4. Hydraulic coupling meso parameters when simulating the deviator stress axial strain curves of Liu et al. [10]

| Parameter name | Conductivity coefficient (mm/s) | Apparent volume of domain (m ³) | Pipe diameter (mm) | Time step | Head pressure (MPa) |
|----------------|---------------------------------|---|--------------------|-----------|---------------------|
| Fish symbol | perm | bulk_w | ap_zero | flow_dt | p_given |
| Analog value | 0.01 | 1e-6 | 0.1 | 1.0e-4 | 1 |

When simulating the partial stress axial strain curve of Liu *et al.* [10], the seepage water pressure is 1 MPa, the initial confining pressure at unloading is 15 MPa, and the axial stress level at unloading is 70% of the compressive strength at the time of conventional triaxial loading seepage coupling. The comparison between the numerical simulation results and the test results is shown in Fig. 11.

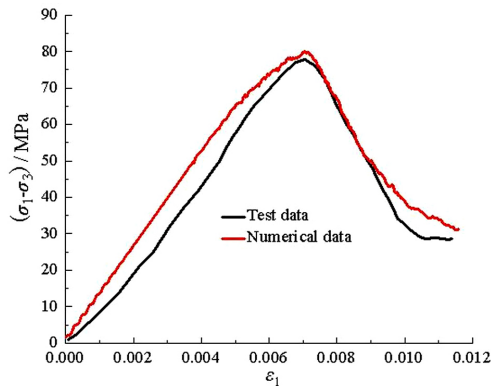


Fig. 11. Comparison of numerical simulation results and test results when simulating the deviator stress axial strain curve of Liu et al. [10]

The test results are in good agreement with the numerical simulation results when the deviator stress-axial strain curves under the coupling of loading and unloading seepage is simulated. Therefore, the particle flow program in this paper can better simulate the mechanical characteristics of rock under the hydraulic coupling.

4. Numerical simulation analysis of rock like structure with cracks under the coupling of loading-unloading and seepage

4.1. Calculation parameters

During the numerical simulation analysis of rock like with cracks under the coupling action of loading and unloading seepage, the basic meso mechanical parameters of particles of rock like samples are shown in Table 5, and the fluid meso mechanical parameters of rock like samples are shown in Table 6.

Table 5. Basic micromechanical parameters of particles in rock like samples

| Model State | Contact modulus of particle (GPa) | Normal tangential stiffness ratio of particle | Coefficient of particle friction | Density of particle (kg/m ³) | Porosity | Average normal strength of parallel bonding (MPa) | Average tangential strength of parallel bonding (MPa) |
|-------------|-----------------------------------|---|----------------------------------|--|----------|---|---|
| saturated | 5.0 | 1.6 | 0.18 | 2700 | 0.08 | 23.32 | 10.05 |

Table 6. Fluid meso mechanical parameters of rock like samples

| Conductivity (mm/s) | Head pressure (MPa) | Pipe diameter (mm) | Fluid bulk modulus K_f (GPa) | Time step (s) | Pipe diameter expansion multiplier (g) |
|---------------------|---------------------|--------------------|--------------------------------|----------------------|--|
| 0.01 | 1, 4, 7 | 1.0 | 2.0 | 1.0×10^{-4} | 1.0×10^3 |

4.2. Numerical simulation analysis of load seepage coupling test results

Taking intact rock like samples and rock like samples with inclined angle of prefabricated crack of 45° as examples, the numerical simulation of load seepage coupling test is carried out. The confining pressure is 10 MPa, and the seepage pressure is 1, 4 and 7 MPa. The deviator stress-strain relationship curves of the load seepage coupling test are shown in Fig. 12.

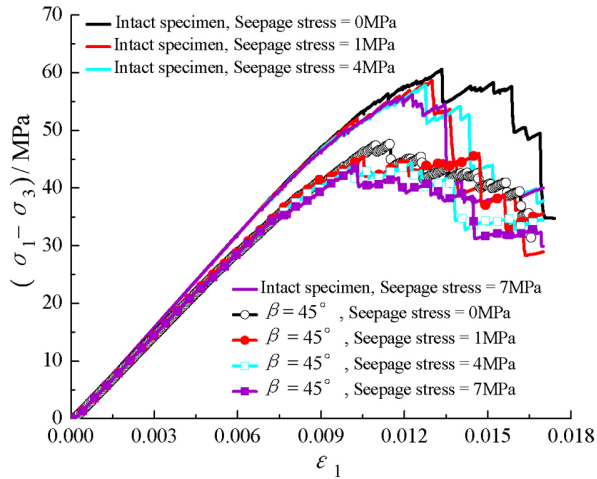


Fig. 12. The deviator stress-strain relationship curves of the load seepage coupling test

Under the action of water pressure, the compressive strength of the intact rock like specimen and the rock like specimen with cracks decreases, and with the increase of water pressure, the compressive strength of the specimen decreases gradually, mainly because water has a certain expansion effect on the cracks.

4.3. Numerical simulation analysis of unloading seepage coupling test results

Taking the rock like sample with inclined angle of crack of 45° as an example, the numerical simulation of unloading seepage coupling test is carried out. The confining pressure is 10 MPa and the osmotic pressure is 4 MPa. Parameter *n* is defined as the ratio of the axial stress during unloading to the compressive strength during the corresponding conventional triaxial loading seepage coupling. Parameter *n* includes three types, i.e. 60%, 70% and 80%. The influence of the initial axial stress on the deviator stress-strain relationship curve of the unloading seepage coupling test is shown in Fig. 13.

When the inclined angle of fracture is the same, the seepage pressure is the same, and the confining pressure is the same, the strength of the specimen also increases with the increase of the initial axial stress level during unloading.

The effect of seepage pressure on the stress-strain curve of rock like specimen with inclined angle of fracture of 45° is analyzed. The confining pressure is 10 MPa, the osmotic pressure is 1, 4 and 7 MPa, and the parameter *n* is 70%. The influence of osmotic pressure on the deviator stress-strain relationship curve of unloading seepage coupling test is shown in Fig. 14.

When the confining pressure is the same, inclined angle of fracture is the same, and the initial axial stress level is the same when unloading, the strength of the specimen decreases gradually with the increase of seepage pressure.

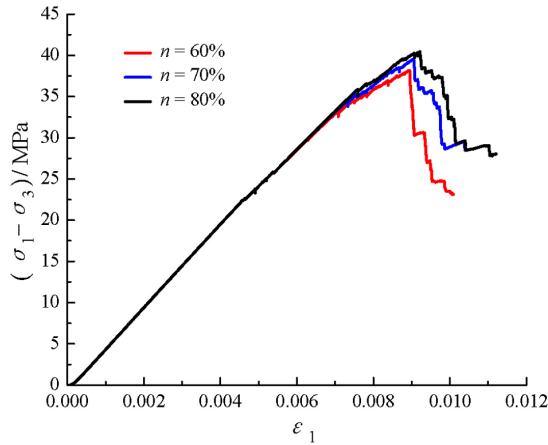


Fig. 13. Effect of initial axial stress on deviator stress-strain curve of unloading seepage coupling test

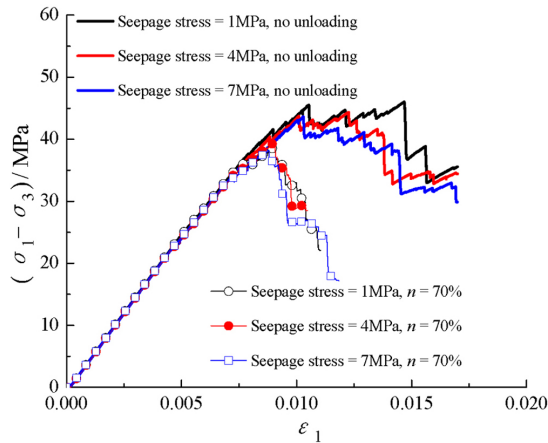


Fig. 14. Effect of osmotic pressure on the deviator stress-strain curve of unloading seepage coupling test

4.4. Comparison of the microcracks of the specimen under loading unloading seepage coupling

Taking the intact sample as an example, the distribution of microcracks in the sample under loading seepage coupling is shown in Fig. 15, and the distribution of microcracks of the sample under unloading seepage coupling is shown in Fig. 16.

In Fig. 15 and 16, the red broken line represents the microcracks, and the blue dot represents the osmotic pressure. When the confining pressure and the osmotic pressure are the same, the unloading effect makes the crack development of the specimen faster and more complete, the specimen is more fragmented and multiple parallel shear bands develop.

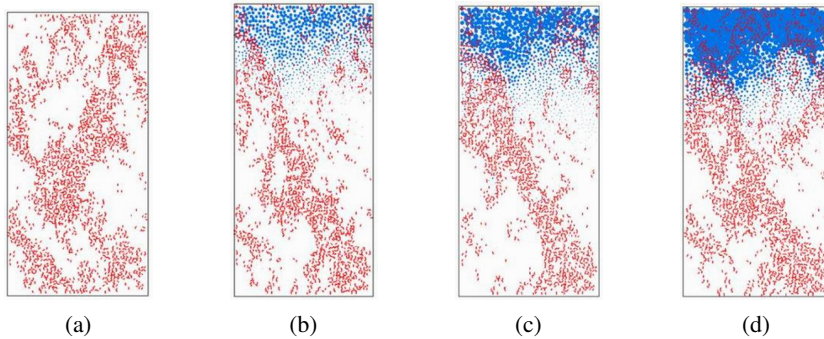


Fig. 15. Distribution of microcracks in the specimen under the coupling of loading and seepage; (a) Seepage stress = 0 MPa, (b) Seepage stress = 1 MPa, (c) Seepage stress = 4 MPa, (d) Seepage stress = 7 MPa

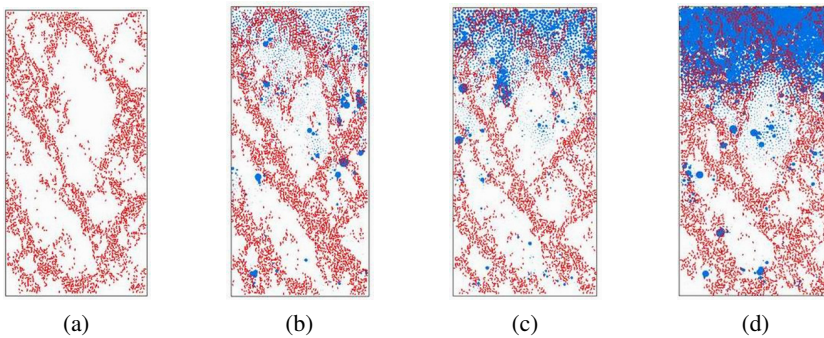


Fig. 16. Distribution of microcracks in the specimen under unloading seepage coupling; (a) Seepage stress = 0 MPa, (b) Seepage stress = 1 MPa, (c) Seepage stress = 4 MPa, (d) Seepage stress = 7 MPa

5. Conclusions

1. When PFC is used for numerical simulation of seepage stress coupling, the conductivity coefficient k can be taken as 0.010. When the pipe diameter is 1.0 mm, the apparent volume of the current domain is $1 \times 10^{-6} \text{ m}^3$, the water pressure distribution inside the sample is relatively uniform. The influence of time step on the peak strength and peak strain of the specimen can be almost ignored.
2. Under the action of water pressure, the compressive strength of the intact rock like specimen and the rock like specimen with cracks decreases, and the compressive strength of the specimen decreases gradually with the increase of water pressure. When the inclined angle of fracture is the same, the seepage pressure is the same, and the confining pressure is the same, the strength of the specimen also increases with the increase of the initial axial stress level during unloading.

3. When the confining pressure and the osmotic pressure are the same, the unloading effect makes the crack development in the specimen faster and more complete, the specimen is more fragmented and multiple parallel shear bands develop.

Acknowledgements

This work was supported by the Open Research Fund of Hunan Provincial Key Laboratory of Hydropower Development Key Technology (Grant No. PKLHD202002), the Open Research Fund of State Key Laboratory of Geohazard Prevention and Geoenvironment Protection (Grant no. SKLGP2021K020) and the Open Research Fund of Engineering Research Center of Underground Mine Construction, Ministry of Education (Grant No. JYBGCZX2020101).

References

- [1] P. Besuelle, G. Viggiani, J. Desrues, et al., “A laboratory experimental study of the hydromechanical behavior of boom clay”, *Rock Mechanics and Rock Engineering*, vol. 47, pp. 143–155, 2014, doi: [10.1007/s00603-013-0421-8](https://doi.org/10.1007/s00603-013-0421-8).
- [2] C.L. Zhang and T. Rothfuchs, “Experimental study of the hydro-mechanical behaviour of the Callovo-Oxfordian argillite”, *Applied Clay Science*, vol. 26, no. 1–4, pp. 325–336, 2004, doi: [10.1016/j.clay.2003.12.025](https://doi.org/10.1016/j.clay.2003.12.025).
- [3] D.S. Yang, S. Chanchole, P. Valli, et al., “Study of the anisotropic properties of argillite under moisture and mechanical loads”, *Rock Mechanics and Rock Engineering*, vol. 46, no. 2, pp. 247–257, 2013, doi: [10.1007/s00603-012-0267-5](https://doi.org/10.1007/s00603-012-0267-5).
- [4] J. Yu, X. Chen, Y.Y. Cai, et al., “Triaxial test research on mechanical properties and permeability of sandstone with a single joint filled with gypsum”, *KSCE Journal of Civil Engineering*, vol. 20, pp. 2243–2252, 2016, doi: [10.1007/s12205-015-1663-7](https://doi.org/10.1007/s12205-015-1663-7).
- [5] Z.X. Ning, Y.G. Xue, Z.Q. Li, et al., “Damage characteristics of granite under hydraulic and cyclic loading–unloading coupling condition”, *Rock Mechanics and Rock Engineering*, vol. 55, pp. 1393–1410, 2020, doi: [10.1007/s00603-021-02698-3](https://doi.org/10.1007/s00603-021-02698-3).
- [6] S.L. Liu, Q.Z. Zhu, and J.F. Shao, “Deformation and mechanical properties of rock: effect of hydromechanical coupling under unloading conditions”, *Bulletin of Engineering Geology and the Environment*, vol. 79, pp. 5517–5534, 2020, doi: [10.1007/s10064-020-01824-9](https://doi.org/10.1007/s10064-020-01824-9).
- [7] X. Chen, C.A. Tang, J. YU, et al., “Experimental investigation on deformation characteristics and permeability evolution of rock under confining pressure unloading conditions”, *Journal of Central South University*, vol. 25, pp. 1987–2001, 2018, doi: [10.1007/s11771-018-3889-2](https://doi.org/10.1007/s11771-018-3889-2).
- [8] C. Zhang and L. Zhang, “Permeability characteristics of broken coal and rock under cyclic loading and unloading”, *Natural Resources Research*, vol. 28, pp. 1055–1069, 2019, doi: [10.1007/s11053-018-9436-x](https://doi.org/10.1007/s11053-018-9436-x).
- [9] F.D. Zhang, “Research on rock permeability and failure characteristics under different loading and unloading paths”, *Acta Geophysica*, vol. 70, no. 3, pp. 1363–1371, 2022, doi: [10.1007/s11600-022-00788-6](https://doi.org/10.1007/s11600-022-00788-6).
- [10] X.R. Liu, J. Liu, D.L. Li, et al., “Unloading mechanical properties and constitutive model of sandstone under different pore pressures and initial unloading levels”, *Journal of China Coal Society*, vol. 42, no. 10, pp. 2592–2600, 2017 (in Chinese).

Received: 2023-06-20, Revised: 2023-12-05